

The Use of Cavitating Jets to Oxidize Organic Compounds in Water

K. M. Kalumuck
Principal Research Scientist

G. L. Chahine
President

DYNAFLOW, Inc.,
7210 Pindeil School Rd.,
Fulton, MD 20759
e-mail: info@dynaflo-inc.com

Exposure to ultrasonic acoustic waves can greatly enhance various chemical reactions. Ultrasonic acoustic irradiation of organic compounds in aqueous solution results in oxidation of these compounds. The mechanism producing this behavior is the inducement of the growth and collapse of cavitation bubbles driven by the high frequency acoustic pressure fluctuations. Cavitation bubble collapse produces extremely high local pressures and temperatures. Such conditions are believed to produce hydroxyl radicals which are strong oxidizing agents. We have applied hydrodynamic cavitation to contaminated water by the use of submerged cavitating liquid jets to trigger widespread cavitation and induce oxidation in the bulk solution. Experiments were conducted in recirculating flow loops using a variety of cavitating jet configurations and operating conditions with dilute aqueous solutions of p-nitrophenol (PNP) of known concentration. Temperature, pH, ambient and jet pressures, and flow rates were controlled and systematically varied. Samples of the liquid were taken and the concentration of PNP measured with a spectrophotometer. Experiments were conducted in parallel with an ultrasonic horn for comparison. Submerged cavitating liquid jets were found to generate a two order of magnitude increase in energy efficiency compared to the ultrasonic means. [S0098-2202(00)00303-5]

Introduction

Ultrasonic cavitation is known (Brown and Goodman [1]) to produce sonochemically activated reactions in water resulting in the formation of highly effective oxidizing hydroxyl radicals. Usually this is achieved using ultrasonic horns that send a high intensity acoustic beam into the solution and excite microcavities. Such systems have been found to promote a wide range of chemical reactions (Suslick [2]) and to be capable of oxidizing dilute aqueous mixtures of organic compounds. However, such devices essentially self limit the efficiency of the process by achieving cavitation only in a thin layer near the surface of the sonifer. In addition, the efficiency of the transfer of electric power into ultrasonic waves into the liquid is known to be quite low—of the order of 15–20 percent.

We employ a mechanism for generating cavitation in a wide body of the liquid by an array of submerged cavitating jets. This process can be made very efficient and benefits in addition from the fact that pumps are quite efficient (of the order of 75 percent) at converting electric (or other) power into hydraulic power. A system based on this technology would be relatively inexpensive, and could be designed into a low-energy technology that will perform at an optimum level creating fast degradation of toxic substances without generating carcinogenic materials such as can occur with chlorination.

Dissociation of Water and Release of Oxidizing Radicals

Exposure to ultrasonic waves can drive many chemical reactions through the generation, growth, and subsequent collapse of cavitation bubbles (e.g., Brown and Goodman [1], Suslick [2]). It is universally accepted that this cavitation with its accompanying local high pressures and temperatures drives these reactions rather than the acoustic waves themselves. The acoustic waves provide a means for transferring the energy of the acoustic driver to cavitation nuclei whose subsequent behavior converts this energy to pressure, heat, erosion, chemical reaction, etc.

When subjected to cavitation, water undergoes dissolution according to the following chemical reaction (e.g., Suslick [3], Neppiras [4])



The free hydroxyl radical $\text{OH} \cdot$ is one of the most powerful oxidizing agents and is an excellent initiator of chain reactions. Oxidation of organic compounds results in various intermediate and end products depending on the compound. These include water vapor, carbon dioxide, inorganic ions and short chain inorganic acids (e.g., see Suslick [2]; Hua et al. [5]; Skov et al. [6]). Often the intermediate products also undergo subsequent oxidation. Modeling of radical production due to cavitation bubble collapse has recently been performed by Gong and Hart [7].

Under the oscillating pressure field of an ultrasonic horn or due to large fluctuating pressure forces in the shear layer of a cavitating and resonating jet, pre-existing microscopic bubble nuclei in the liquid grow and collapse. There are several competing theories for the predominant phenomena that triggers the anomalous chemistry present during the bubble collapse. According to one, the generation of a “hot spot” upon bubble collapse (local high temperature and pressure region) is responsible for the phenomena (Neppiras [4]; Suslick et al. [8]; Suslick et al. [9]). Others suggest that the reactions are due to shock waves or electric discharges generated at the collapse and the fragmentation (Margulis [10]) or to the plasma like state generated in the collapsing bubble (LePoint and Mullie [11]).

Recently, a number of researchers have looked into using ultrasound to degrade organic contaminants. The list is too extensive to review here. However, a sample of relevant work includes that of Hua et al. [5,12], Kotronarou et al. [13,14], Cheung et al. [15], and Hua and Hoffman [16]. Such work has been performed in both batch and continuous flow modes using ultrasonic horns and plates. Also recently, a commercial scale process has been employed utilizing a venturi type cavitation flow loop often in combination with UV irradiation and hydrogen peroxide addition (U.S. Environmental Protection Agency [17]; Skov et al. [6]).

Cavitation Bubble Dynamics. In a pressure field, a bubble works as an oscillator with the gaseous contents acting as a spring

Contributed by the Fluids Engineering Division for publication in the JOURNAL OF FLUIDS ENGINEERING. Manuscript received by the Fluids Engineering Division October 14, 1999; revised manuscript received May 3, 2000. Associate Technical Editor: J. Katz.

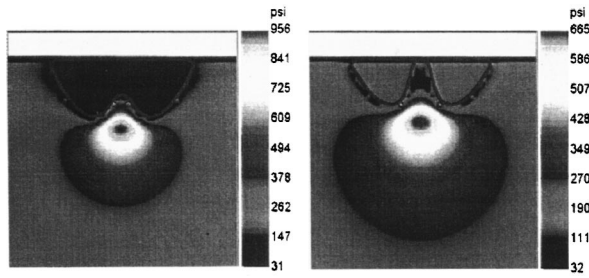


Fig. 1 Pressure field associated with nonspherical bubble collapse. Taken from Chahine and Duraiswami [19]

and the inertia being provided by the motion of the surrounding liquid. Under external pressure forcing, the bubble undergoes volume and shape oscillations. As the bubble compresses the inside pressure grows.

For a collapsing spherical cavity in a liquid of density ρ under external steady pressure P_{amb} , and with gas inside the bubble having a specific heat ratio k , Neppiras [4] has shown that as the bubble collapses, a very high pressure region is generated near the bubble wall in the liquid with a maximum pressure P_{max} given by

$$P_{max} = P_{g0} \left[\frac{P_{amb}(k-1)}{P_{g0}} \right]^{k/(k-1)}, \quad (2)$$

where p_{g0} is the initial gas pressure in the bubble. For a value of $k=4/3$ he obtained the corresponding temperature

$$T_{max} = T_0 \left(\frac{P_{amb}}{3p_{g0}} \right). \quad (3)$$

With $P_{amb}=1$ atm, and $p_{g0}=0.01$ atm, the maximum pressure may be as high as 1.2×10^4 atm, and the temperature could be as high as $10,000^\circ K$ (Young [18]). Thus extremely high values of temperature and pressure are generated in a small region of space where the bubble collapse occurs. Such physical conditions could explain the enhancement by cavitation of the chemical dissociation of the aqueous medium releasing hydroxyl radicals.

However, cavitation bubbles rarely behave spherically. Typically, due to initial or boundary condition asymmetries and to bubble interacting, the bubble, upon collapse, forms a high speed reentering jet (Young [18]; Chahine and Duraiswami [19]). Figure 1 presents a calculation we have performed for a bubble collapsing near a solid wall and forming a high speed jet which impacts the wall. Visible in the figure are the very high pressures in the liquid near the jet (Chahine and Duraiswami [19]). Such computations show the potential for extremely high pressures not only in the gas inside the bubble but also in a focused area of the liquid. In practice, bubbles often occur in "clouds" in which bubble/bubble interaction and bubble deformation effects occur (Chahine [20]; Chahine and Duraiswami [21]). In cavitating jets, elongated, rotating, and ring shaped bubble cavities form which have also been found to collapse with the formation of reentering jets (Chahine and Johnson [22]; Chahine and Genoux [23]).

Cavitating Water Jets. Cavitating water jet technology represents one successful attempt to harness and utilize the destructive power of cavitation. Various means and nozzle designs can be used to induce the explosive growth of microscopic cavities or bubbles within a liquid jet. Moving away from the orifice region, these bubbles encounter higher pressures and collapse. For example, by inserting a solid surface in front of the nozzle at an appropriate distance, nozzle generated cavities can be induced to collapse violently on that surface in the high-pressure stagnation region of the jet so created (Johnson et al. [24]; Chahine and Johnson [22]; Chahine et al. [25]).

Cavitating jets have the following advantages over ultrasonic devices.

- 1 The cavitation can be made to be much more intense and aggressive.
- 2 The location of the cavitation "center" can be more easily controlled, and multiple centers in a small volume can be easily provided.
- 3 From a practical standpoint, a jet based process is simpler, more flexible, easily scaled up and able to process larger industrial level quantities of liquid for a given power input.
- 4 As demonstrated in this paper, the jets are significantly more efficient.

The dimensionless parameter characterizing cavitation is the cavitation number, σ ,

$$\sigma = \frac{P_{amb} - p_v}{1/2 \rho V^{*2}} \approx \frac{P_{amb} - p_v}{\Delta P}, \quad (4)$$

where ρ is the liquid density, V^* is the characteristic flow velocity, and ΔP is the pressure drop across the nozzle. The particular value at which cavitation is incipient σ_i is termed the cavitation inception number. Thus if the operating conditions for a submerged jet are such that $\sigma/\sigma_i < 1$, cavitation will occur, and as σ/σ_i continues to decrease below unity the amount of cavitation will increase.

Experimental Setup

Experiments were conducted in several jet flow loops and in an ultrasonic system. Preliminary investigations were conducted in a cavitation reaction chamber constructed of plexiglass to enable viewing of the cavitation and flow. Due to the potential for many organic compounds to attack plexiglass this cell was not used for actual oxidation tests. Instead, jet cavitation reactors constructed of stainless steel were utilized.

One loop was driven by a triplex positive displacement pump which produced a flow of 4.5 gpm at pressures up to 1000 psi. The flow from the pump was sent to a multi-stage cavitation reaction chamber. Each stage included a jet orifice plate with multiple orifices and a stagnation plate located downstream of the orifice plate and designed to stagnate the jet flows thereby inducing strong bubble collapse. A second was driven by a centrifugal pump capable of 56 gpm at up to 75 psi and is shown in the sketch of Fig. 2. The loop was fabricated of steel piping. Upon exiting the pump, the liquid flowed into a pipe manifold into which a large number of orifices had been machined. The total fluid volume of this loop was 6.5 liters. Reservoir temperature was maintained at the desired value by use of a cooling loop inside the reservoir and immersion of the reservoir in a large tank filled with water and containing a refrigeration coil.

Ultrasonic Setup. A sketch of the ultrasonic device is provided in Fig. 3. The device is driven by magnetostrictive oscillations produced in a nickel stack surrounded by electromagnetic

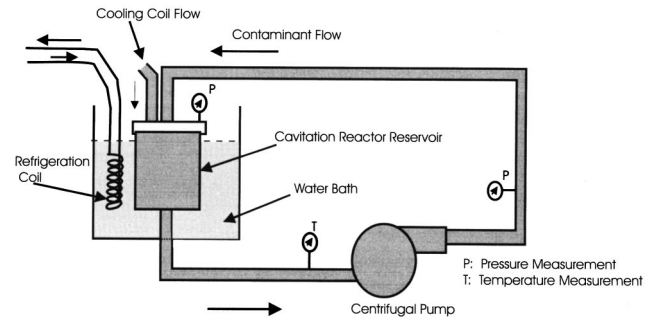


Fig. 2 Sketch of jet loop capable of 56 gpm at 60 psi

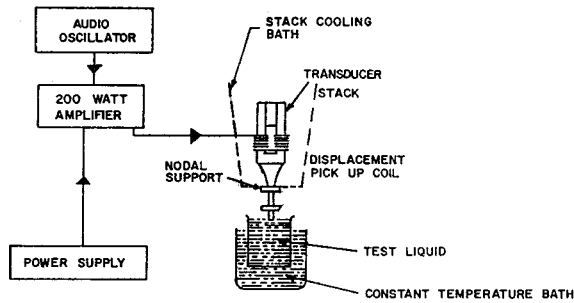


Fig. 3 Sketch of ultrasonic experimental setup

coils. The oscillations are amplified by a tapered titanium horn tuned to resonate at 15.7 kHz. The waveform is produced by a frequency generator and amplified before being fed to the coils. A 3/8 in. diameter titanium "button" or "tip" was attached to the end of the horn. The amplitude of oscillation of the tip was initially calibrated using a bifilar microscope. Its amplitude was monitored during testing by a sensor whose voltage output is proportional to displacements. The tip displacement amplitude was set to 0.0026 in. peak to peak.

The horn tip was submerged 0.125 in. in a 150 ml glass beaker filled with 25 ml of test sample liquid. Initially, the submergence was varied, and the value of 0.125 in. was selected because it produced the greatest amount of cavitation. The top of the beaker was covered with a plastic sheet through which the horn was inserted. The sample beaker was surrounded with a cooling bath to maintain a constant temperature.

Measurement Techniques and Procedures. Reagent grade p-Nitrophenol—"PNP"—(Aldrich, 99 percent), phosphoric acid (Aldrich, 85 percent), and sodium hydroxide (VWR Scientific, 1.0 N) were used. The PNP was in crystalline form and was mixed with distilled water.

PNP concentrations were measured using a UV-Vis spectrophotometer following the procedures of Kotronarou et al. [13] and Hua et al. [12]. The spectrophotometer was calibrated against known concentrations of PNP in distilled water at a wavelength of 400 nm after shifting the sample pH to 11 by the addition of NaOH to enable measurement employing the absorption band at 400 nm.

During testing, 3 ml samples were drawn from the test reservoir. Following the addition of NaOH, the sample was drawn through a Gelman 0.2 micron PTFE syringe filter to remove any particulate contaminants such as titanium erosion particles from the ultrasonic tests. The filtered sample was then placed in the spectrophotometer and its transmittance measured.

Uncertainty Estimates. The estimated uncertainty in measured quantities are: flow rate, ± 5 percent; pressure, ± 1 psi; concentration, ± 0.2 ppm; pH, ± 0.2 ; temperature, $\pm 1^\circ\text{F}$. The oxidation efficiency (defined in Eq. (5)) and the nondimensional concentration, C/C_0 are derived quantities. Their estimated uncertainties are: oxidation efficiency, ± 10 percent; C/C_0 , ± 4 percent.

Results and Discussion

Performance Evaluation: Oxidation Efficiency. A key measure of the performance of the oxidation process is the energy required to remove a unit mass of a given compound. For overall performance, this can be expressed as the cumulative mass of contaminant removed per unit energy expended. When plotted against time, this represents a running value of the efficiency. We define this to be the *oxidation efficiency* given by

$$m^*(t) = \frac{(C_0 - C(t)) * \mathcal{V}}{t * \mathcal{P}} \quad (5)$$

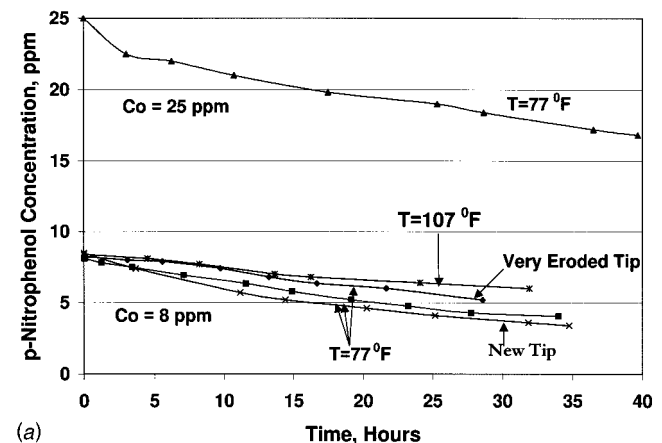
Table 1 Comparison of power densities for PNP oxidation experiments

	watts/ml	Type
Ultrasonic	0.36	Batch
Cavitating Jets	0.18-12	Continuous flow

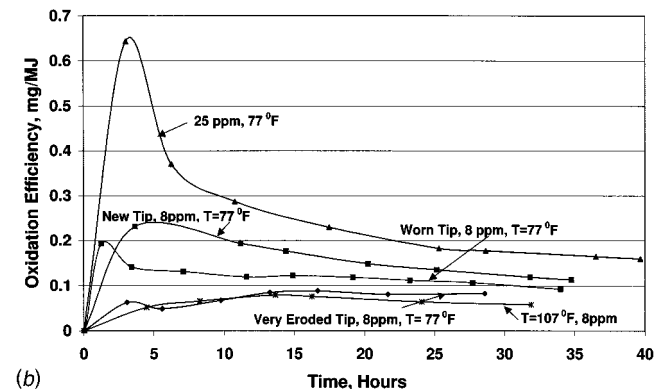
Here, C_0 is the initial concentration, $C(t)$ the concentration at time t , \mathcal{V} the liquid volume, and \mathcal{P} the power expended. The peak value in the curve of $m^*(t)$ can be used to characterize the peak performance of each system.

The power used in this efficiency calculation is that which is imparted to the liquid. For the jet process, it is simply based on the hydraulic power imparted by the pump. For the ultrasonic horn, it is the acoustic energy dissipated in the liquid which was determined with a calorimetric test by measuring the heat generated. This enables use of the "oxidation efficiency" as a measure of the efficiency of the particular configuration for the cavitation phenomenon and removes variations in power consumption due to varying pump, motor, or horn configurations. The actual amount of energy that must be supplied to a system employing either the ultrasonic or jet induced cavitation is therefore larger due to these conversion inefficiencies. The ranges of the power input to the liquid per unit volume (power density) we utilized are shown in Table 1.

Ultrasonic Tests. Sample results of ultrasonic tests of the oxidation of PNP are presented in Fig. 4. Figure 4 presents the measured concentrations as a function of time for several cases run at a pH of 3.5 and initial concentrations of 8 and 25 ppm for comparison with the jet oxidation studies. We did not seek to



(a)



(b)

Fig. 4 Ultrasonic sonication of PNP at pH=3.5. Top: concentration versus time. Bottom: oxidation efficiency.

optimize the conditions for the ultrasonic horn since this has been experimentally investigated for aqueous solutions of PNP by others (Kotronarou et al. [13], Hua et al. [5,12]). We selected conditions from the literature which were near optimal. These tests were run at 77°F and 107°F with the rate of oxidation lower at 107°F than at 77°F—consistent with the general behavior of sonochemical reaction rates as described in Suslick [2]. Direct comparison of these results with those in the literature can be done using oxidation rates normalized with applied power. Normalization of results with the applied power shows that our results are comparable to those in the literature; e.g., the oxidation rate of Kotronarou et al. [13] is 0.89 mg/MJ. Calorimetric measurements showed that approximately 18 percent of the electric power input to the horn was converted to acoustic power and dissipated as heat in the liquid.

Cavitating Jet Results. Figure 5 presents sample results of the oxidation of PNP with submerged cavitating jets conducted in the flow loop of Fig. 2. The operating temperature was 107°F which, as described below, was found to produce the best performance. The pH was comparable to that of the ultrasonic tests of Fig. 4, and the initial concentration, 8 ppm, was used in the majority of the cases in Fig. 4. We can compare the oxidation efficiencies in Figs. 4 and 5 for achieving a given decrease in PNP concentration. For example, a 50 percent reduction (from 8 ppm to 4 ppm) is achieved by the jet system in 1.5 hrs. while the ultrasonic horn requires approximately 30 hrs. The corresponding oxidation efficiency for the cavitating jets (3 mg/MJ) is about 25

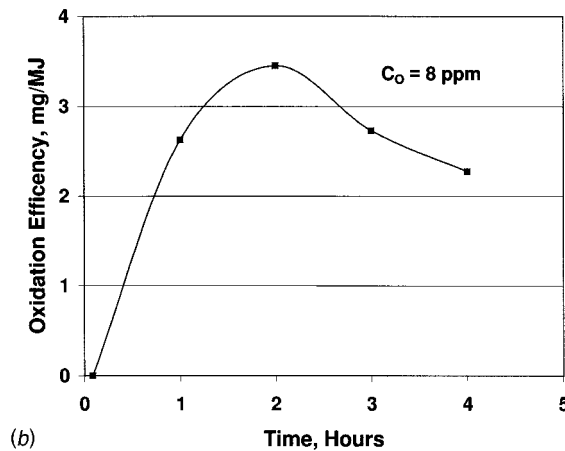
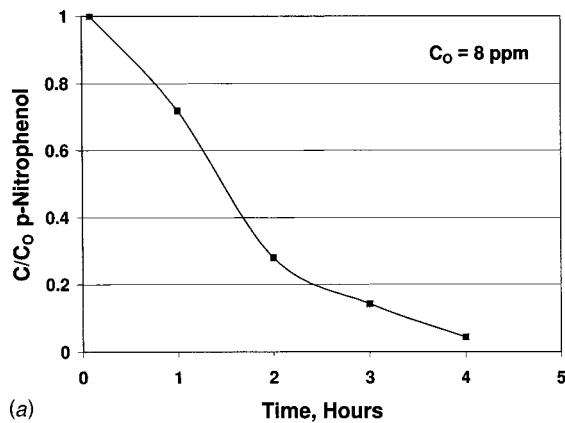


Fig. 5 Cavitating jet oxidation of PNP: pH=3.8, T=107°F, ambient pressure=20 psia, pressure entering nozzles =75 psia, flow rate=57 gpm, $C_0=8$ ppm. Top: time variation of the ratio of PNP concentration to its initial value. Bottom: oxidation efficiency.

times larger than that of the ultrasonic device (0.12 mg/MJ). While the investigations conducted have not as yet been of sufficient scope to state that either the jet or ultrasonic devices are operating at their optima, a range of parameters have been investigated in the current study for the jets and in the literature for the ultrasonic device. The conditions of Figs. 4 and 5 are near the best known for each device. If the differences in conversion efficiency of input power to power into the liquid (e.g., 18 percent for ultrasonic, approximately 75 percent for a motor/pump) were used, an additional factor of 4 would need to be applied, and the cavitating jet results would exhibit overall energy efficiencies 100 times higher than the ultrasonic device. This suggests strong promise for application of jet cavitation to oxidation.

Temperature Effect. The results of the experiments of jet oxidation of PNP indicated the existence of an optimal temperature or temperature range for oxidation efficiency. Figure 6 shows the influence of temperature on the oxidation efficiency at three times during the oxidation process. Performance is seen to be best at the intermediate temperature range near 42°C (107°F). Such behavior is consistent with cavitation erosion intensity which is known to achieve a maximum value that is temperature and liquid dependent. For water at atmospheric pressure, this peak is at approximately 50°C (122°F) (Brown and Goodman [1]). Above this temperature the bubble dynamics becoming increasingly thermally controlled rather than inertially controlled which leads to an increase in vapor pressure and cushioning of the bubble collapse.

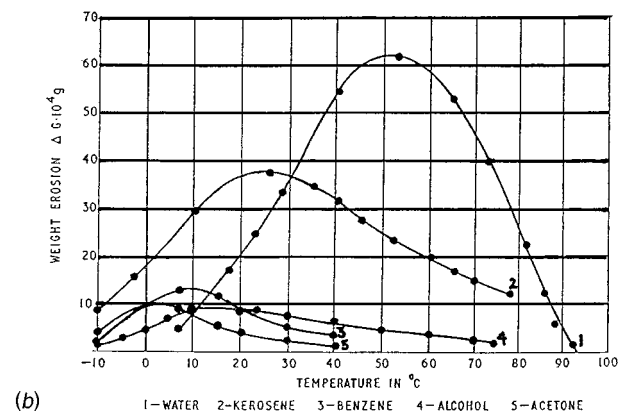
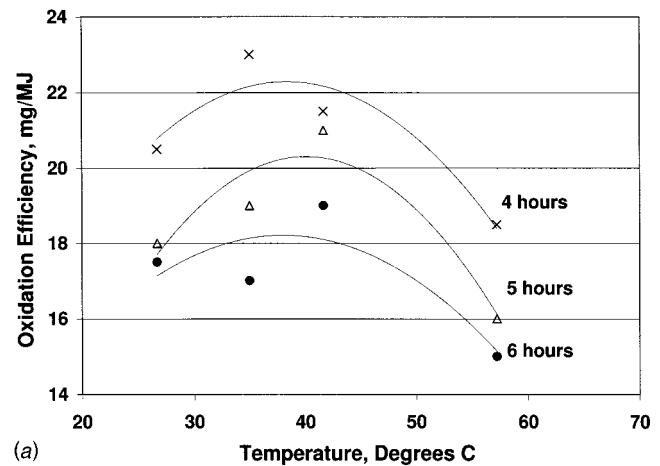


Fig. 6 Influence of temperature on cavitation effects exhibiting a region of maximum influence. (a) Jet oxidation efficiency of PNP at 4, 5, and 6 hours of operation; pH=3.8, ambient pressure=21 psia, pressure entering nozzles=70 psi. (b) Erosion of aluminum as a function of temperature for various liquids; taken from Brown and Goodman [1].

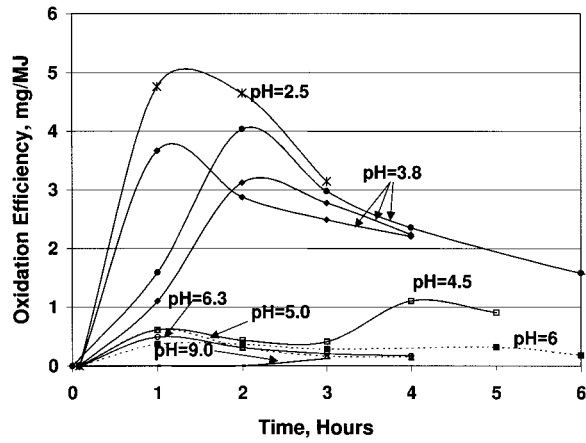


Fig. 7 Influence of pH on jet oxidation efficiency of PNP: T=107°F, ambient pressure=20 psia, pressure entering nozzles=75 psia

pH Effect. The values of pH in the flow loops were adjusted periodically to their set point values by the addition of phosphoric acid or sodium hydroxide. The pH was typically maintained within ± 0.3 . Figure 7 provides the results of operation at varying pH. The oxidation efficiencies are seen to strongly depend on pH in a nonlinear fashion with little influence for pH above about 4. As the pH decreases below 4, the rate is found to increase, initially at long times and then at shorter times for decreasing pH. The data of Kotronarou et al. [13] with PNP using an ultrasonic device showed similar behavior.

To assure that our increased efficiencies with decreased pH was indeed due to the cavitation oxidation and not solely to pH, a sample of the PNP solution was adjusted to a pH of 2.5 and left to sit for 4 days. Measurement of the PNP concentration after 4 days showed no change from the initial measurement.

Influence of Cavitation Number. The effects of cavitation number were studied by changing the ambient pressure while maintaining the pressure drop across the nozzle constant. The results are presented in Fig. 8 for two values of the cavitation number. The lower cavitation number shows a significant increase in degradation rate which can be explained by the creation of a larger volume of cavitation created with lower power.

Ring Vortex Cavities. A simple analysis based on jet cavitation occurring in vortical structures is now presented. A cavitating and structured jet can be considered as being formed of a succession of vortex bubble rings of diameter equal to the orifice diam-

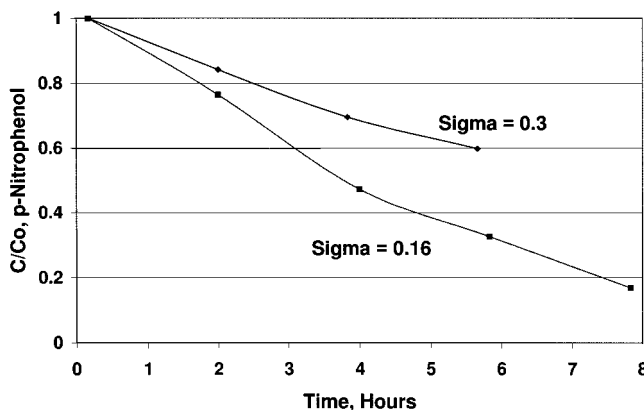


Fig. 8 Influence of cavitation number, sigma, on jet oxidation of PNP: pH=3.8, T=107°F

eter D_0 . The cavitation intensity per unit time, I_{cav} , can be expressed as the product of the number of cavitation events per unit time, N , and the collapse energy of each cavitation event, E_{bub} ,

$$I_{cav} = NE_{bub} \quad (6)$$

The cavity potential energy E_{bub} can be expressed as the product of its maximum volume and the pressure difference between the surrounding liquid and the cavity contents which we will approximate as the ambient pressure, P_{amb} . For ring cavities, with a maximum cross-section radius R_{max} ,

$$E_{bub} = \pi^2 D_0 R_{max}^2 P_{amb} \quad (7)$$

For a ring emission frequency, f , for each of n nozzles, I_{cav} , is given by

$$I_{cav} = fnE_{bub} \quad (8)$$

Using the product of the pressure and flow for hydraulic power, the energy conversion efficiency, η , can be taken as:

$$\eta = \frac{fnE_{bub}}{1/2\rho V_{jet}^2 Q} = \epsilon^2 2\pi \frac{S_d P_{amb}}{\rho V_{jet}^2} = \epsilon^2 2\pi S_d \sigma \sim \epsilon^2, \quad (9)$$

where ϵ and the jet Strouhal number S_d are defined as:

$$\epsilon = \frac{2R_{max}}{D_0}, \quad S_d = \frac{fD_0}{V_{jet}} \cong 0.3. \quad (10)$$

The volume fraction of liquid cavitated, α , is the ratio of the volume of all ring cavities at their maximum size created during a unit time, V_{cav} , and the flow rate Q :

$$\alpha = \frac{V_{cav}}{Q} = \frac{4\pi R_{max}^2 f}{D_0 V_{jet}} = \pi S_d \epsilon^2 \sim \epsilon^2. \quad (11)$$

We see that the parameters α and η both increase strongly with ϵ . This is illustrated by the results of Kalumuck et al. [26], which showed, based on numerical simulations using a vortex ring cavity dynamics model (Chahine and Genoux [23]; Genoux and Chahine [27]), that ϵ increases with lower ambient pressures thus increasing both the volume fraction of fluid cavitated and the efficiency of conversion of hydraulic energy to cavity collapse energy.

Conclusions

Experiments to establish the feasibility of utilizing cavitating jets for oxidation of organic compounds in dilute aqueous solutions were carried out in recirculating flow loops. Baseline tests were conducted with an ultrasonic device for comparison. Results were consistent with those of the literature. Cavitating jet oxidation of p-nitrophenol was found to exhibit a two order of magnitude increase in energy efficiency compared to ultrasonic means. The data indicate an inverse relation of efficiency with cavitation number which is consistent with the results of a simple jet cavitation model. An optimal temperature for cavitating jet oxidation may be that for peak erosion rates due to cavitation. As with ultrasonic results of the literature, cavitating jet oxidation rates improved with decreasing pH.

These results suggest a great potential for the use of jet cavitation in full scale waste treatment and remediation systems.

Acknowledgments

The authors wish to thank Gary Frederick and Patrick Aley of DYNFLOW for conducting the experiments and Dr. Nail Gumerov of DYNFLOW for discussions and modeling efforts. The authors also wish to thank Drs. Lawrence Principe of the Johns Hopkins University, Inez Hua of Purdue University, Alan Brause of ACSC, and Andrew Alpert of PolyLC for a number of helpful discussions and consultations. This work was sponsored in part by NSF under SBIR award No. DMI-9661572.

References

- [1] Brown, B., and Goodman, J. E., 1965, *High Intensity Ultrasonics*, Van Nostrand, Inc., Princeton, NJ.
- [2] Suslick, K. S., ed., 1988, *Ultrasonics, Its Chemical, Physical, and Biological Effects*, VCH, New York.
- [3] Suslick, K. S., 1989, "Sonochemistry," *Science*, **247**, pp. 1439–1445.
- [4] Neppiras, E. A., 1980, "Acoustic Cavitation," *Phys. Rep.*, **61**, pp. 159–251.
- [5] Hua, I., Hochemer, R., and Hoffman, M., 1995, "Sonochemical Degradation of p-Nitrophenol in a Parallel Plate Near Field Acoustic Processor," *Environ. Sci. Technol.*, **29**, pp. 2790–2796.
- [6] Skov, E., Pisani, J., and Beale, S., 1997, "Cavitation Induced Hydroxyl Radical Formation," American Institute of Chemical Engineering National Meeting, Houston, TX.
- [7] Gong, C., and Hart, D. P., 1998, "Ultrasound Induced Cavitation and Sonochemical Yields," *J. Acoust. Soc. Am.*, **104**, No. 4, pp. 2675–2682.
- [8] Suslick, K. S., Cline, Jr., R. E., and Hammerton, D. A., 1986, "The Sonochemical Hot Spot," *J. Am. Chem. Soc.*, **108**, p. 5641.
- [9] Suslick, K. S., Doktycz, S. J., and Flint, E. B., 1990, "On the Origin of Sonoluminescence and Sonochemistry," *Ultrasonics*, **28**, pp. 280–290.
- [10] Margulis, M. A., 1990, "The Nature of Sonochemical Reactions and Sonoluminescence," *Adv. Sonochem.*, **1**, pp. 39–81.
- [11] LePoint, T., and Mullie, F., 1994, "What Exactly is Cavitation Chemistry?" *Ultrason. Sonochem.*, **1**, pp. 13–22.
- [12] Hua, I., Hochemer, R., and Hoffman, M., 1995, "Sonolytic Hydrolysis of p-Nitrophenyl Acetate: The Role of Supercritical Water," *J. Phys. Chem.*, **99**, pp. 2335–2342.
- [13] Kotronarou, A., Mills, G., and Hoffman, M., 1991, "Ultrasonic Irradiation of p-Nitrophenol in Aqueous Solution," *J. Phys. Chem.*, **95**, pp. 3630–3638.
- [14] Kotronarou, A., Mills, G., and Hoffman, M., 1992, "Decomposition of Parathion in Aqueous Solution by Ultrasonic Irradiation," *Environ. Sci. Technol.*, **26**, pp. 1460–1462.
- [15] Cheung, H. M., Bhatnagar, A., and Jansen, G., 1991, "Sonochemical Destruction of Chlorinated Hydrocarbons in Dilute Aqueous Solution," *Environ. Sci. Technol.*, **25**, p. 1510.
- [16] Hua, I., and Hoffman, M., 1996, "Kinetics and Mechanism of the Sonolytic Degradation of CCl₄: Intermediates and Byproducts," *Environ. Sci. Technol.*, **30**, pp. 864–871.
- [17] U. S. Environmental Protection Agency, 1994, "CAV-OX Cavitation Oxidation Process Magnum Water Technology, Inc. Applications Analysis Report," U.S. Environmental Protection Agency Report EPA/540/AR-93/520.
- [18] Young, F. R., 1989, *Cavitation*, McGraw-Hill, London.
- [19] Chahine, G. L., and Duraiswami, R., 1994, "Boundary Element Method for Calculating 2D and 3D Underwater Explosion Bubble Behavior in Free Water and Near Structures," U. S. Naval Surface Warfare Center Technical Report NSWCDD/TR-93/44.
- [20] Chahine, G. L., 1991, "Dynamics of the Interaction of Non-Spherical Cavities," *Mathematical Approaches in Hydrodynamics*, Miloh, T., ed., SIAM, Philadelphia.
- [21] Chahine, G. L. and Duraiswami, R., 1992, "Dynamical Interactions in a Bubble Cloud," *ASME J. Fluids Eng.*, **114**, No. 4, pp. 680–686.
- [22] Chahine, G. L., and Johnson, V. E., Jr., 1985, "Mechanics and Applications of Self-Resonating Cavitating Jets," *International Symposium on Jets and Cavities*, ASME, WAM, Miami, FL.
- [23] Chahine, G. L., and Genoux, Ph., 1983, "Collapse of a Cavitating Vortex Ring," *ASME J. Fluids Eng.*, **105**, pp. 400–405.
- [24] Johnson, V. E., Kohn, R. E., Tiruvengadam, A., and Conn, A. F., 1972, "Tunneling, Fracturing, Drilling, and Mining with High Speed Water Jets Utilizing Cavitation Damage," *Proceedings, 1st International Symposium on Jet Cutting Technology*, Coventry, U.K.
- [25] Chahine, G. L., Kalumuck, K. M., and Frederick, G. S., 1995, "Cavitating Water Jets for Deep Hole Drilling in Hard Rock," *Proceedings, 8th American Water Jet Conference*, Houston, TX, Vol. 2, pp. 765–778.
- [26] Kalumuck, K. M., Chahine, G. L., Frederick, G. S., Aley, P. D., Brittain, W. L., and Gumerov, N. A., 1997, "Oxidation of Organic Compounds in Water with Cavitating Jets," DYNALFLOW, INC. Technical Report 97002-Insf.
- [27] Genoux, Ph. and Chahine, G. L., 1984, "Simulation of the Pressure Field Due to a Submerged Oscillating Jet Impacting on a Solid Wall," *ASME J. Fluids Eng.*, **106**, 491–496.